International Journal of Nanomedicine

Dovepress
open access to scientific and medical research

Open Access Full Text Article

ORIGINAL RESEARCH

Contrast-enhanced MR imaging of atherosclerosis using citrate-coated superparamagnetic iron oxide nanoparticles: calcifying microvesicles as imaging target for plaque characterization

This article was published in the following Dove Press journal:
International Journal of Nanomedicine
19 February 2013
Number of times this article has been viewed

Susanne Wagner[1]
Jörg Schnorr[1]
Antje Ludwig[2]
Verena Stangl[2]
Monika Ebert[1]
Bernd Hamm[1]
Matthias Taupitz[1]

[1]Department of Radiology, Section of Experimental Radiology, Charité – Universitätsmedizin Berlin, Campus Charité Mitte, and Campus Benjamin Franklin, Berlin, Germany; [2]Department of Cardiology, Section of Experimental Cardiology, Charité – Universitätsmedizin Berlin, Campus Charité Mitte, Berlin, Germany

Objective: To evaluate the suitability of citrate-coated very small superparamagnetic iron oxide particles (VSOP) as a contrast agent for identifying inflammation in atherosclerotic lesions using magnetic resonance imaging (MRI).

Methods and results: VSOP, which have already been evaluated as a blood pool contrast agent for MR angiography in human clinical trials, were investigated in Watanabe heritable hyperlipidemic rabbits to determine to what extent their accumulation in atherosclerotic lesions is a function of macrophage density and other characteristics of progressive atherosclerotic plaques. In advanced atherosclerotic lesions, a significant MRI signal loss was found within 1 hour after intravenous administration of VSOP at the intended clinical dose of 0.05 mmol Fe/kg. Histological examinations confirmed correlations between the loss of MRI signal in the vessel wall and the presence of Prussian blue-stained iron colocalized with macrophages in the plaque cap, but surprisingly also with calcifying microvesicles at the intimomedial interface. Critical electrolyte magnesium chloride concentration in combination with Alcian blue stain indicates that highly sulfated glycosaminoglycans are a major constituent of these calcifying microvesicles, which may serve as the key molecules for binding VSOP due to their highly complexing properties.

Conclusion: Calcifying microvesicles and macrophages are the targets for intravenously injected VSOP in atherosclerotic plaques, suggesting that VSOP-enhanced MRI may render clinically relevant information on the composition and inflammatory activity of progressive atherosclerotic lesions at risk of destabilization.

Keywords: atherosclerosis, inflammation, magnetic resonance imaging, iron oxide nanoparticles, glycosaminoglycans, calcifying microvesicles

Introduction

Experimental and clinical studies show that intravenously (IV) administered polymer-stabilized ultrasmall iron oxide nanoparticles (USPIO; eg, ferumoxtran-10, DDM 43/34, P904) accumulate in areas of inflammatory activity within atherosclerotic lesions.[1–5] This accumulation is seen as a loss of signal on magnetic resonance imaging (MRI). USPIO accumulation is based on phagocytosis by macrophages, which are an accepted imaging target for visualizing inflammation of the vessel wall.[3–10] Hence USPIO accumulation may be a suitable target for assessing the risk of plaque rupture by noninvasive MRI.[1,3–5,9] Available preclinical studies and clinical trials in humans suggest that the optimal time for detecting the MRI signal loss induced in

Correspondence: Matthias Taupitz
Klinik für Radiologie, Charité – Universitätsmedizin Berlin, Campus Benjamin Franklin, Hindenburgdamm 30, 12203 Berlin, Germany
Tel +49 030 844 530 41
Fax +49 030 450 752 7953
Email matthias.taupitz@charite.de

atherosclerotic lesions using dextran- or other polymer-coated USPIO (eg, ferumoxtran-10, ferumoxytol, or P904), is 24 to 48 hours after IV administration.[3–5,11–13] This is clearly not optimal for ensuring a smooth workflow in the routine clinical setting. Several cell culture studies have shown that cellular uptake of citrate-coated iron oxide nanoparticles is faster and quantitatively superior to that of polymer-coated iron oxide nanoparticles.[14,15] Therefore, we investigated the accumulation of intravenously injected citrate-coated very small superparamagnetic iron oxide particles (VSOP) in atherosclerotic lesions of Watanabe heritable hyperlipidemic (WHHL) rabbits using ex vivo MRI and histology. Histologic evaluation included not only macrophages but also calcifying microvesicles, which have recently been identified as a cofactor in plaque thrombogenicity, plaque inflammatory burden, plaque rupture, and plaque calcification.[16–19]

Methods

Contrast medium

Citrate-coated VSOP (batch 050701, VSOP C184) were provided by Ferropharm GmbH (Teltow, Germany). The batch used in this study is identical to the batch used in the Phase I and Phase II clinical trials.[20,21] VSOP have been described in detail elsewhere.[20,22] Briefly, their basic properties are: a core diameter of 4 nm; hydrodynamic diameter of 7 nm; T1-relaxivity of 18.7; and T2-relaxivity of 30 L/(mmol × seconds) at 0.47 T. VSOP are stabilized with citrate, an anionic monomeric coating. The concentration of the active substance is 27.9 g Fe/L, which corresponds to 0.5 mol Fe/L. For optimal biological safety and tolerability, the citrate iron oxide dispersion was pharmaceutically formulated with mannitol (6 g/L), meglumine (2 g/L), and glycerphosphate (2 g/L) as the excipients to adjust pH, osmolality, and dispersion stability.

Animals and anesthesia

The animal experiments were approved by the Landesamt für Gesundheit und Soziales (LAGeSo), Berlin, Germany (G0263/01). Five WHHL rabbits (Charles River AG, Sulzfeld, Germany) were examined at the age of 18–20 months. One animal served as a control and was sacrificed without contrast medium administration. Four rabbits received VSOP at a dose of 0.05 mmol Fe/kg body weight (BW); two rabbits were sacrificed 1 hour after administration, and two rabbits were sacrificed 24 hours after administration. Four chinchilla bastard rabbits (Charles River AG) aged 18 months served as atherosclerosis-free controls, each receiving 0.05 mmol Fe/kg BW of the above-described VSOP and were sacrificed 1 hour after administration. Aortas were removed and processed as described in the Supplementary materials.

Ex vivo MRI

Agar phantoms with aortic rings were imaged ex vivo on a whole body MR scanner at a field strength of 1.5 T (Magnetom Sonata; Siemens AG, Erlangen, Germany) using a commercially available extremity coil. The phantoms were imaged with frontal section orientation, resulting in axial images of the aortic rings, using a two-dimensional T2*-weighted fat-suppressed gradient recalled echo sequence (TR 150 ms/TE 11 ms/flip angle 40°, eight averages) with 1.5 mm slice thickness and 0.31 × 0.31 mm in-plane resolution.

Histology

The aortic rings were removed from the ex vivo MRI phantom and embedded in paraffin, aligning the aortic rings in such a way as to enable the correlation of histology and MRI. The paraffin blocks were cut into 5 µm sections, which were mounted on SuperFrost Ultra Plus slides (Menzel GmbH, Braunschweig, Germany). The following staining procedures were performed in serial sections (for a detailed description of staining procedures see the Supplementary materials): Movat pentachrome, von Kossa, alizarin (pH 11), alizarin S (pH 4.2 and 6.4), Prussian blue, anti-rabbit macrophage (anti-RAM-11), anti-smooth muscle cell actin (anti-SMA), and anti-vascular endothelial growth factor (anti-VEGF). In selected specimens containing a large number of so-called calcifying microvesicles, a critical electrolyte concentration Alcian stain was performed according to the method of Scott and Dorling.[23,24]

Evaluation

Ex vivo MRI

MRI signal intensities in up to 16 circumferential segments of each aortic ring were measured quantitatively (SI_{raw}) in regions of interest positioned in cap, intima, and media using a free software tool (OsiriX Imaging Software; Pixmeo SARL, Bernex, Switzerland) on an Apple Mac OS × 10.5 desktop computer (Apple Inc, Cupertino, CA, USA). To compensate for coil- and B1-field-related MRI signal intensity inhomogeneities within the MRI field of view, a reference MRI signal intensity from the agar (SI_{agar}) close to the region of interest of each aortic ring segment was measured. These data served to calculate relative MRI signal intensities for each aortic ring segment and within each aortic ring segment for each vessel wall layer:

$$SI_{rel} = SI_{raw}/SI_{agar}. \quad (1)$$

Correlation of ex vivo MRI and histology

The aortic ring specimens of all WHHL rabbits showed a broad intraindividual distribution of pathologic features such as calcification, presence of macrophages, and loss of smooth muscle cells in the media, and therefore also a wide range of types of atherosclerotic lesions according to the definition of the American Heart Association (AHA).[25] A correlation of MRI signal intensities and pathological features was obtained by histological segmentation of the vessel rings on the basis of contiguous microscopic fields of view in a 200-fold magnification (Figure 1A–C). Each microscopically defined field of view segment was matched with a corresponding segment of the aortic ring in ex vivo MRI. Each field of view segment was evaluated for the following pathological features using a score-based semiquantitative approach: AHA type using the classification of Stary et al[25] and modified by Virmani et al[26] (as shown in Table S1), count of calcifying microvesicles, anti-RAM positive spots, anti-VEGF positive spots, anti-SMA positive cell layers, Alcian blue positive microvesicles, and Prussian blue positive spots and cells. Score definitions are presented in Table S2.

Statistical analysis

The analysis included the ex vivo MRI signal intensities and the results of the histologic examinations. Individual view segments were regarded as cases independent of the animals from which they originated. Statistical analysis was performed with the Statistical Package for the Social Sciences ([SPSS] IBM Corporation, Armonk, NY, USA). Results were calculated as the mean ± standard deviation. Statistical differences were assessed with the Mann–Whitney U-test. For correlation analysis of MRI signal intensities with pathological features, Kendall's tau-b was calculated. Two-sided *P*-values less than 0.05 were regarded as statistically significant.

Results

View-segment-based evaluation resulted in 439 view segments from 41 aortic rings in WHHL rabbits with VSOP, in 95 view segments from eight aortic rings in the WHHL rabbit without VSOP, and in 104 view segments from 14 aortic rings from control rabbits with VSOP injection. There was no significant difference in distribution of AHA types between view segments of WHHL rabbits with VSOP and the WHHL rabbit without VSOP. There was also no difference in the distribution of AHA types between the view segments of WHHL rabbits sacrificed 1 hour and 24 hours after VSOP administration. There was also no difference in signal loss between 1 and 24 hours after VSOP injection based on a statistical comparison of AHA types. Therefore, data on both time points were pooled for further statistical analysis.

AHA type and MRI signal intensities

Areas of markedly low MRI signal intensity in the vessel wall were only seen in aortic rings of the four WHHL rabbits treated with IV VSOP (Figure 2A–H). With increasing AHA lesion type in the range of 0 to 5B, but with the exception of the fibrotic lesion type 5C, the relative MRI signal intensities decreased in both groups (ie, those with and without VSOP administration; Figure 3). For AHA lesion types 4, 5A, and 5B, the relative MRI signal intensities were significantly lower in the group with VSOP administration compared

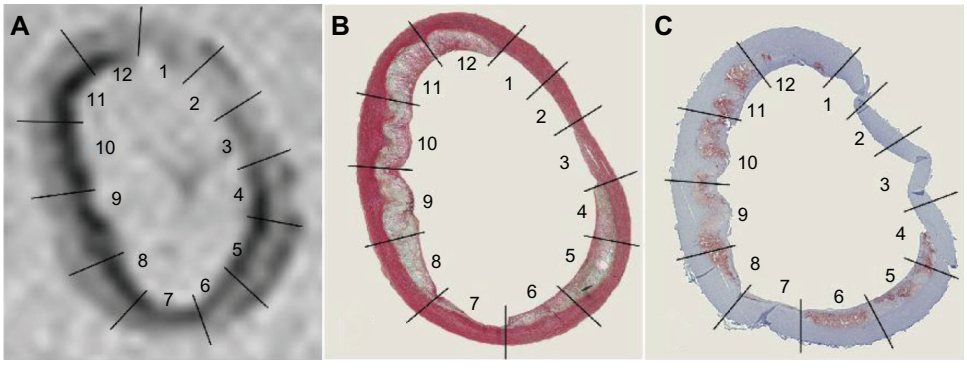

Figure 1 Ex vivo MRI of an aortic ring of a WHHL rabbit 1 hour after administration of VSOP at a dose of 0.05 mmol Fe/kg BW (**A**). Corresponding histological specimens stained with Movat pentachrome (**B**) and anti-rabbit macrophage RAM-11 with hematoxylin counterstain (**C**).

Notes: Straight lines confine the corresponding view segments. The Movat pentachrome stain demonstrates the presence of different AHA types within one aortic ring with healthy and intact arterial wall in segments 1–3 and advanced lesion types in segments 8–12. The inner diameter of the aortic ring shown here is 3.8 mm by 6.1 mm with a wall thickness between 0.4 mm and 1.3 mm (in-plane resolution of this GRE T2*-weighted image is 0.31 × 0.31 mm).

Abbreviations: MRI, magnetic resonance imaging; WHHL, Watanabe heritable hyperlipidemic; VSOP, very small superparamagnetic iron oxide particles; BW, body weight; AHA, American Heart Association; GRE, gradient recalled echo.

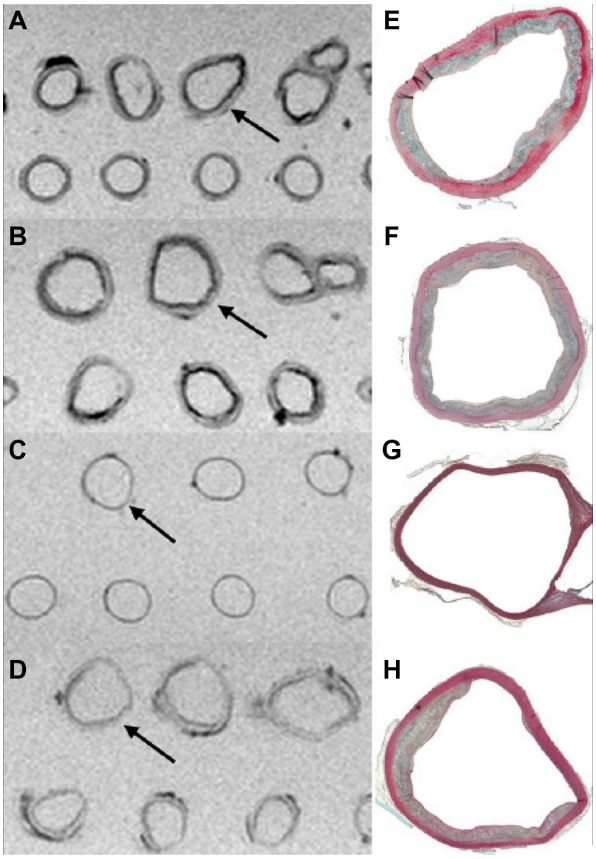

Figure 2 Ex vivo MRI of aortic rings in an agar matrix (two-dimensional T2*-weighted fat-suppressed GRE sequence, TR 150 ms/TE 11 ms/flip angle 40°) in comparison to histologic specimens (Movat pentachrome stain). Aortic rings from WHHL rabbit 1 hour (**A**) and 24 hours (**B**) after intravenous administration of VSOP at a dose of 0.05 mmol Fe/kg BW show irregular areas of low MRI signal intensity, which were not observed in aortic rings from the chinchilla bastard rabbit (control without atherosclerosis) with VSOP injection (**C**) and the WHHL rabbit without VSOP injection (**D**). Arrows indicate the corresponding aortic ring in the histological specimen (**E**–**H**). There were no differences between intravenous injection after 1 or 24 hours regarding MRI signal intensities induced by VSOP. Areas of low MRI signal intensity in the aortic rings in (**D**) correspond to fatty tissue and calcifications.

Abbreviations: MRI, magnetic resonance imaging; GRE, gradient recalled echo; TR, repetition time; TE, echo time; WHHL, Watanabe heritable hyperlipidemic; VSOP, very small superparamagnetic iron oxide particles; BW, body weight.

to the group without VSOP (Figure 3). In WHHL rabbits with VSOP injection, fibrotic lesions of type 5C were not associated with significantly different MRI signal intensities compared to type 1–3 lesions. In summary, these results suggest that VSOP injection is associated with a diagnostically relevant MRI signal loss in progressive advanced AHA lesion types, enabling their differentiation from fibrotic lesion types, which show only minor MRI signal loss.

Prussian blue iron stain and MRI signal intensities

Only in WHHL rabbits with VSOP injection and in view segments with advanced lesion types were Prussian blue-positive deposits found, indicating an accumulation of VSOP: (1) in endothelial cells and in subendothelial cell layers colocalized with macrophages (Figure 4A and B); (2) as Prussian blue-positive microvesicles (Figure 5A); and (3) in or between medial cell layers (Figure 4C). No Prussian blue-detectable iron was found in atherosclerotic lesions of the WHHL rabbit without VSOP injection (Figure S1A). The view-segment-based evaluation demonstrates a correlation for low MRI signal intensities with high Prussian blue score in the cap (Figure 6A; Kendall's tau-b, –0.378; $P < 0.01$) and in the intima (Figure 6B; Kendall's tau-b, –0.562; $P < 0.01$). In the media, the Prussian blue scores were negligible.

von Kossa calcium stain and MRI signal intensities

In the WHHL rabbits, calcifications were found solely in association with microvesicles in most of the view segments (Figure 5B). These calcified microvesicles were abundant in the intimomedial region of most of the view segments. Only in a few aortic rings additional calcifications were found in the subendothelial cell layer (Figure S2A). These calcified subendothelial cells also show an alcianophilia in the Movat stain (Figure S2B). Aortic rings of one WHHL rabbit showed calcification of the medial cell layers (Figure S2C). Low MRI signal intensities correlated with a high von Kossa score in the intima in WHHL rabbits with VSOP (Figure 6C; Kendall's tau-b, –0.221; $P < 0.01$) and without VSOP (Kendall's tau-b, –0.231; $P < 0.01$), which reflects the tendency of calcifications to cause a loss of MRI signal intensity. Nevertheless, MRI signal intensities were significantly lower with VSOP injection for all von Kossa scores.

Alcianophilic microvesicles in Movat stain and MRI signal intensities

In Movat pentachrome stain, deep blue microvesicles were found mainly at the intimomedial interface (Figure 5C). There is a correlation between low MRI signal intensities and high microvesicle scores for the group with VSOP (Figure 6D; Kendall's tau-b, –0.386; $P < 0.01$) as well as for the group without VSOP (Kendall's tau-b, –0.282; $P < 0.01$). For all microvesicle scores, the relative MRI signal intensities are significantly lower in the group with VSOP injection. Qualitatively, it is remarkable that confluent deposits of microvesicles showing deep blue Alcian staining are associated with advanced vessel wall destruction and also with confluent calcifications (Figure S3A and B), which reflects a possible link between alcianophilic tissue components and calcium accumulation.

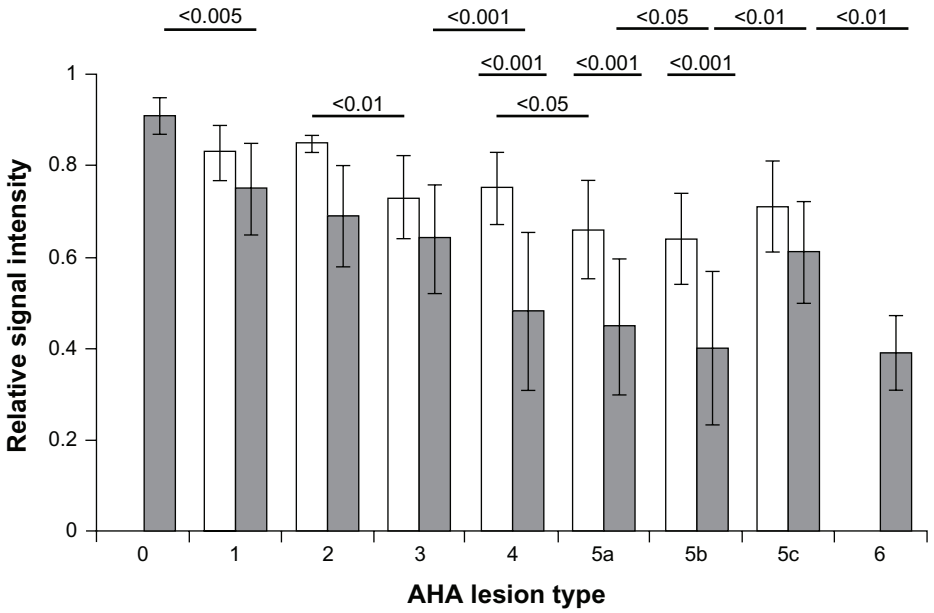

Figure 3 Correlation of MRI signal intensities and AHA plaque types of vessel wall view segments.
Notes: Gray bars, with VSOP; white bars, without VSOP. With the progression of AHA type 0–5B, there is a correlation with a decrease in relative MRI signal intensity in rabbits with VSOP (Kendall's tau-b, –0.278; $P < 0.01$), and as well without VSOP (Kendall's tau-b, –0.366; $P < 0.01$) reflecting an influence of calcification on MRI signal intensities. MRI signal intensities for advanced lesion types 4, 5A, and 5B were significantly lower for the vessel wall segments of rabbits with VSOP compared to the control without VSOP. AHA type 5C reflects a fibrotic stable type with no significant MRI signal decrease with VSOP. *P*-values given above the columns refer to the differences in relative MRI signal intensities compared with the next higher AHA type with VSOP (upper row) and without VSOP (lower row). The middle row provides *P*-values for differences in relative MRI signal intensities between groups with VSOP and without VSOP. There was no segment observed with lesion type 6 in the rabbit without VSOP injection.
Abbreviations: MRI, magnetic resonance imaging; AHA, American Heart Association; VSOP, very small superparamagnetic iron oxide particles.

Anti-RAM-11 macrophage stain and MRI signal intensities

Some aortic rings displayed a perfect match between low MRI signal intensity and anti-RAM 11 stain, as shown in Figure 1A and C. Matches between Prussian blue-positive stain and anti-RAM-11 stain were mainly found in intracellular localization in subendothelial areas and in the shoulder of atherosclerotic lesions. On the other hand, in the intimomedial region the detection of RAM-11 positive cells did not correlate with vessel wall destruction, and often only faint clouds of RAM-11 extracellular material were detectable, which could possibly be attributed to residues of

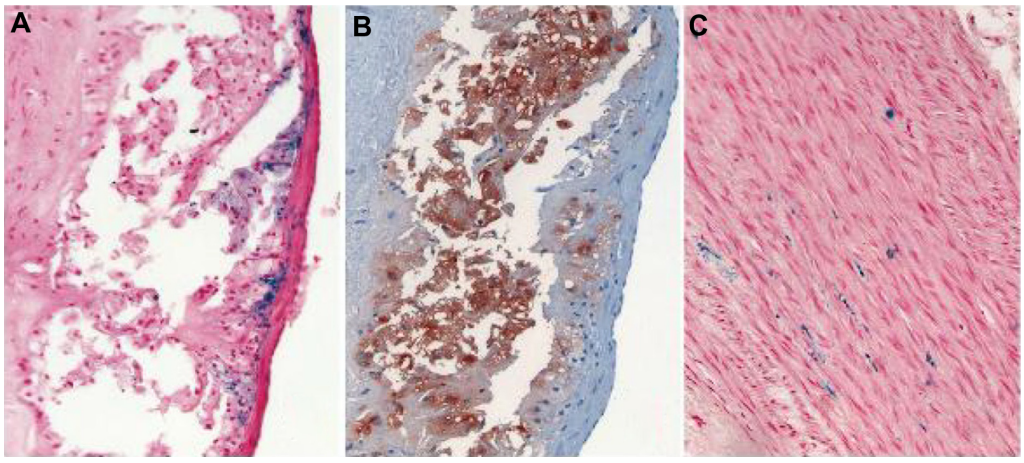

Figure 4 Examples of the localization of Prussian blue-positive deposits in relation to endothelial and subendothelial cells in an advanced lesion of a WHHL rabbit 1 hour after VSOP injection (**A**) in comparison with anti-RAM-11 stain (**B**). Iron deposits in the medial layer of an atherosclerotic vessel wall in a WHHL rabbit 24 hours after VSOP injection (**C**). There was no difference between 1 hour and 24 hours after injection with regard to these patterns.
Abbreviations: WHHL, Watanabe heritable hyperlipidemic; VSOP, very small superparamagnetic iron oxide particles.

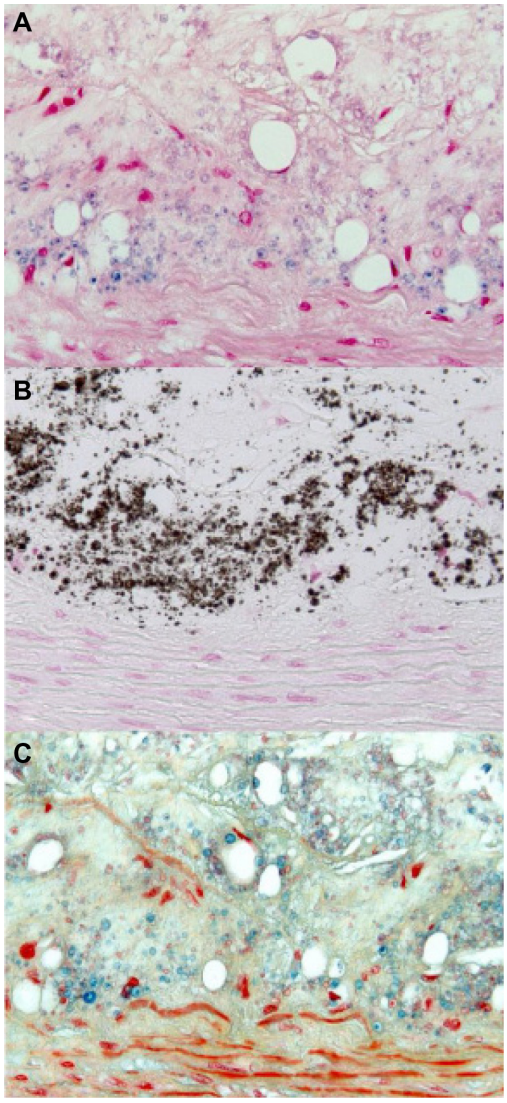

Figure 5 Histology of the intima-media interface of an advanced atherosclerotic lesion classified as AHA type 4. Positive Prussian blue stain (**A**) indicates VSOP iron accumulation in microvesicles, which are colocalized to calcifying microvesicles at the intima-media interface in the von Kossa stain (**B**), and to alcianophilic vesicles in the Movat pentachrome (**C**) stain.
Note: Original magnification 400×.
Abbreviations: AHA, American Heart Association; VSOP, very small superparamagnetic iron oxide particles.

macrophages after apoptotic cell death. Despite the observation that for all anti-RAM scores in the cap and intima, MRI signal intensities were significantly lower with VSOP than without VSOP, there was no correlation for decreasing MRI signal with increasing anti-RAM score, as it was found for the other histological features (Figure 6E and F).

Anti-SMA stain, anti-VEGF stain, and MRI signal intensities

With plaque progression, there was a decrease in anti-SMA-positive cells in the media and an increase in the cap, where anti-VEGF was mainly located intracellularly in smooth muscle cells in the media and as extracellular deposits in the intimomedial area of the atherosclerotic lesions. There was a correlation between low MRI signal intensities and: (1) loss of medial cell layers in rabbits with VSOP injection (Kendall's tau-b, –0,381; $P < 0.01$); (2) increase in anti-VEGF deposits in the intima (Kendall's tau-b, –0.294; $P < 0.01$); and (3) increase in anti-VEGF deposits in the media (Kendall's tau-b, –0.357; $P < 0.01$).

Ultrastructural histology of microvesicles

Adequate fixation using the above-mentioned alcohol fixation technique as recommended by Puchtler et al[27] revealed extraordinary staining patterns of the microvesicles (Figure 7A–F). The ultrastructural pattern with a fried egg shape of microvesicles with different calcium stainings (von Kossa and Alizarin) resembles the pattern of Prussian blue staining and Movat alcianophilia. The intense blue stain in Movat pentachrome and the critical electrolyte concentration Alcian stain indicates the presence of highly sulfated glycosaminoglycans (GAGs) in the microvesicles. Extracellular anti-VEGF-positive granules and diffuse material were found to be colocalized with the microvesicles, but the ultrastructural shape of the VEGF-positive deposits is not identical to calcium, Alcian blue, or Prussian blue stained vesicles (not shown).

Discussion

Our experimental investigation of the accumulation of IV injected electrostatically stabilized iron oxide nanoparticles (VSOP) in atherosclerotic plaques of WHHL rabbits has yielded three major insights: (1) VSOP produce MRI signal loss in atherosclerotic lesions of the vessel wall as early as 1 hour after IV injection; (2) a small dose of VSOP of 0.05 mmol Fe/kg at this time point already induces a significant signal loss in MRI; and (3) histology reveals significant extracellular accumulation of VSOP in microvesicles in atherosclerotic wall lesions both 1 hour and 24 hours after IV injection. All three findings are new compared to experimental results obtained using sterically stabilized magnetic iron oxide nanoparticles (USPIO) for the detection and characterization of atherosclerotic plaques by MRI. With use of sterically stabilized USPIO, it usually takes at least 24 hours after IV injection before sufficient particle accumulation occurs; larger doses of 0.2–1.0 mmol Fe/kg are necessary, and the particles are mainly localized in macrophages.[1,3–5,9,11,13] Similar to these results, we also saw an accumulation of VSOP in macrophages within

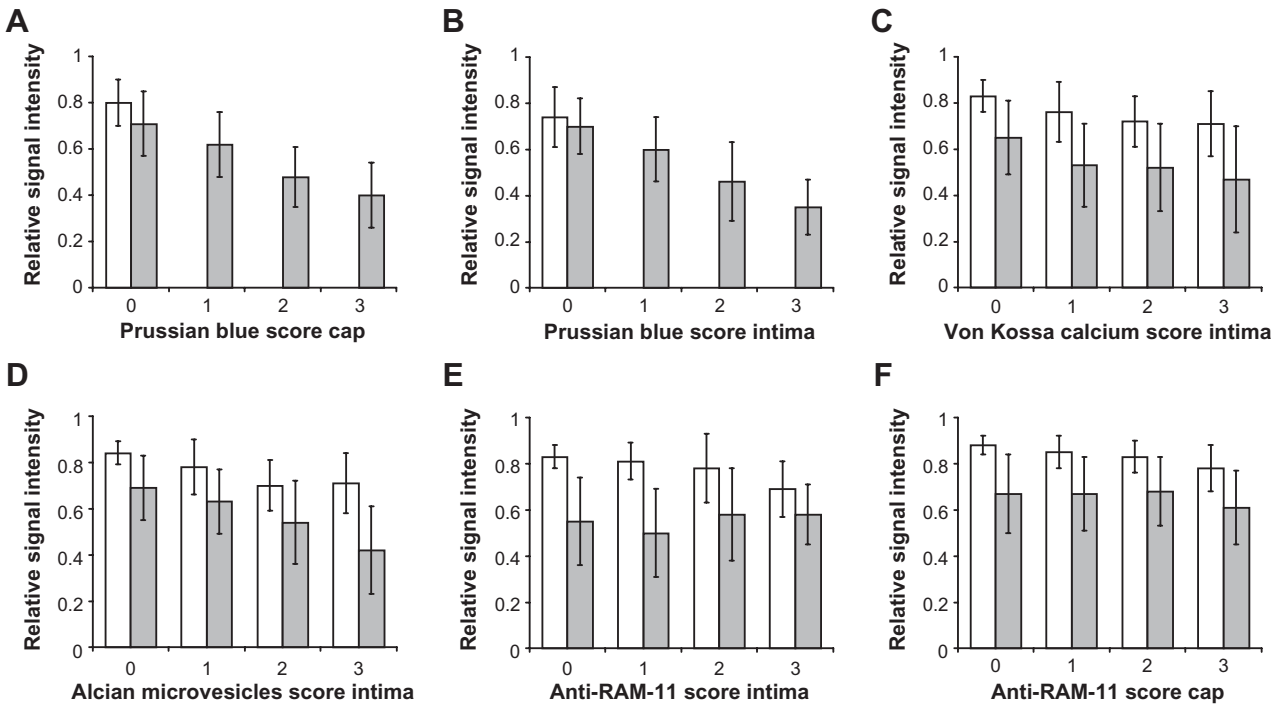

Figure 6 Results of quantitative evaluation of view-segment-based relative MRI signal intensities compared with histological scores for Prussian blue in the cap (**A**), Prussian blue in the intima (**B**), calcifying microvesicles in the intima (**C**), Alcian blue-positive microvesicles in the intima (**D**), anti-RAM-11 in the intima (**E**), and in the cap (**F**).
Notes: Data are shown for corresponding wall layers (cap, intima) for MRI and histological evaluation. MRI signal intensities with VSOP are significantly lower compared to signal intensities without VSOP for all histologic features outlined above.
Abbreviations: MRI, magnetic resonance imaging; VSOP, very small superparamagnetic iron oxide particles.

atherosclerotic lesions. Interestingly, in our study, there was a significant correlation between the amount of positively stained VSOP iron and the corresponding loss of MRI signal and: (1) instability parameters of atherosclerotic plaques based on AHA types, (2) increasing amounts of microvesicles; and (3) increasing scores for calcification; but not (4) with the amount of macrophages. The fact that VSOP accumulate faster in advanced atherosclerotic lesions than sterically stabilized USPIO is attributable to their kinetics. Preclinical and clinical data on these substances show that blood clearance of VSOP is faster compared to sterically stabilized USPIO.[5,20,22,28]

Our findings suggest that microvesicles might be a suitable imaging target for VSOP administered as a contrast medium for the detection and characterization of atherosclerotic plaques by MRI. Microvesicles have recently been proposed to be an important surrogate marker for plaque instability. Li et al[17] found an association of so-called calcifying microvesicles and advanced inflammatory plaque burden in the atherosclerotic lesions of patients with acute myocardial infarction, concluding that these microvesicles indicate plaques with high inflammatory burden regardless of the macrophage cell load. Moreover, microvesicle-like structures as components of necrotic zones of athersoclerotic lesions have been found to be cytotoxic, highly thrombogenic, and promote plaque rupture.[16,18,29] Based on current knowledge, microvesicles are shed by cells such as smooth muscle cells and migrated immune cells, or they are among the myriad of micron-sized vesicles generated in an apoptotic cell explosion.[30] These microvesicles are also referred to as matrix vesicles, microparticles, calcifying vesicles, membrane vesicles, membrane particles, or ceroid vesicles, and it is not yet clear whether there is a single morphological and functional pathological mechanism underlying all of these vesicle types. Our histological examinations show the alcianophilic microvesicles in Movat stain to be identical to the calcifying microvesicles revealed by von Kossa stain.

The histological appearance of the calcifying microvesicles observed in our study reveals a strong positive Alcian dye binding. This is also confirmed by the critical electrolyte staining method at a magnesium chloride concentration of 0.4 M, which provides evidence for the existence of highly sulfated GAGs, which have so far not been discussed as a constituent of the microvesicles. On the other hand, it has been demonstrated using MR spectroscopic measurement that atherosclerotic calcifications are linked to GAGs.[31]

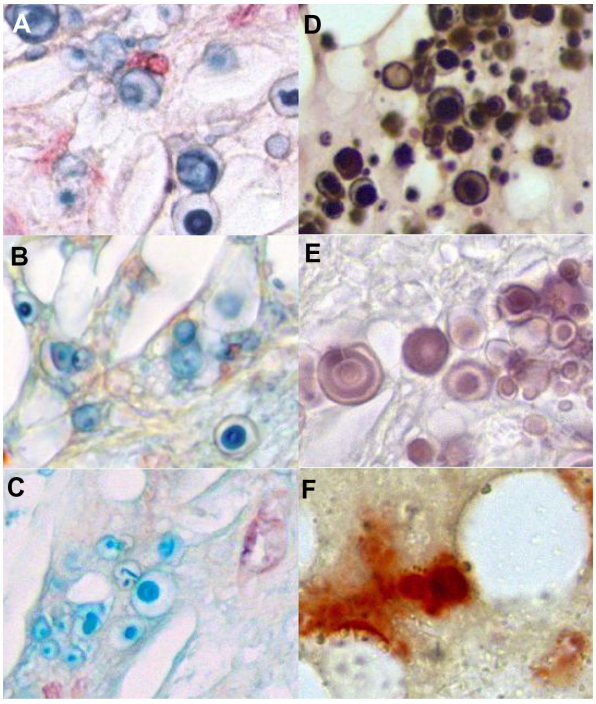

Figure 7 Ultrastructural histology of microvesicles in different stainings. Positive Prussian blue reaction of the microvesicles in a WHHL rabbit with VSOP (**A**). In the Movat pentachrome stain, the microvesicles show a positive Alcian blue reaction indicating GAGs (**B**). The critical electrolyte concentration staining method at 0.4 M magnesium chloride in combination with Alcian blue according to Scott and Dorling[23] indicates the presence of highly sulfated glycosaminoglycans such as heparin, heparin sulfate, or keratan sulfate (**C**). The von Kossa stain reveals a staining pattern comparable to the other staining procedures (**D**). The Alizarin stain at pH 11 as described by Puchtler et al[27] results in more differentiated ultrastructural staining than the von Kossa stain (**E**), whereas the Alizarin S stain at pH 4.2 (**F**) and pH 6.4 (not shown) failed to provide useful results with regard to the differentiation of mircovesicle structures.[27]

Abbreviations: WHHL, Watanabe heritable hyperlipidemic; VSOP, very small superparamagnetic iron oxide particles; GAGs, glycosaminoglycans.

The GAGs are a class of negatively charged carbohydrates based on aminosugar dimers such as uronic or iduronic acid with variable numbers of carboxylic and sulfate moieties, resulting in a negative net charge, which makes them a highly effective cation binder or chelator.

GAGs are well known to interact with iron oxide particle surfaces. For instance, Hale's colloidal iron has been used as a histochemical dye for the detection of GAGs for more than 50 years;[32] coating of iron oxides with chondroitin sulfate or hyaluronic acid results in stable colloids. Regarding the targeting mechanism of VSOP to the microvesicles, we currently assume that in vivo the citrate coating is replaced by the interaction of the iron oxide surface with GAGs due to their higher chelating capacity when compared to citrate.

The involvement of macrophages in atherosclerotic plaque progression makes them an ideal target for the detection of advanced or possibly unstable lesions using USPIO. The lack of a correlation between decreasing MRI signal intensity and increasing anti-RAM staining macrophages in our study using VSOP is not in agreement with published data on the accumulation of USPIO in atherosclerotic lesions. In recently published experimental studies using USPIO, dosages of 0.2–1 mmol Fe/kg BW were administered, leading to a higher saturation of macrophages. However, dosages of iron oxide nanoparticles exceeding 0.075 mmol Fe/kg are not recommended and have not been tested for clinical use. Therefore, within a clinically acceptable dose range, we have to deal with the aspect that not only macrophages but also microvesicles may be an important target for the detection of advanced atherosclerotic lesions using VSOP.

For another USPIO type – polymer-coated iron oxide nanoparticle P904 – Sigovan et al[5] found that the accumulation of Prussian blue-stained iron 24 hours after administration in a rabbit model for atherosclerosis was colocalized with macrophages and extracellular structures, which they could not characterize further.[5] The images of histologic specimens in this publication indicate that these extracellular structures might correspond to microvesicles. The rapid accumulation of VSOP in macrophages and in microvesicles of the vessel wall, which distinguishes them from polymer-coated iron oxides, might be attributable to a more rapid extravasation resulting from the smaller overall particle size of VSOP. Cell culture experiments have also shown that the cellular uptake of VSOP is faster and more effective compared to polymer-stabilized iron oxides, while the mechanism underlying this enhanced accumulation remains to be elucidated.

In addition to suggesting that microvesicles might be a promising imaging target for VSOP at a clinically acceptable dose, our experiments provide new insights into the role and biochemical constitution of microvesicles in atherosclerotic lesion progression, which have to be further investigated.

A further interesting finding of our study is that the degree of accumulation of VSOP in the vessel wall significantly depends on the AHA type of the atherosclerotic plaque and therefore on the degree of vulnerability (instability). Accumulation of VSOP was most pronounced in advanced AHA type 4, 5A, and 5B lesions, where it was scored significantly higher than in the lower-grade AHA types 1–3, and 5C. AHA type 5C corresponds to fibrotic atherosclerotic plaques, which is considered stable due to increased collagen content with less monocyte/macrophage infiltration and fewer debris zones.

Clinical significance

It has previously been shown that VSOP, a member of the group of electrostatically stabilized iron oxide nanoparticles, has the potential to be developed for clinical use, and that

VSOP is an excellent blood pool contrast agent for MR angiography, especially of the coronary arteries.[20,21,33–35] Along with these earlier observations, our experimental evidence of rapid accumulation of IV injected VSOP as a function of histopathologic parameters of plaque instability show that VSOP is a promising candidate for clinical MR angiography and vessel wall imaging; it might allow for the simultaneous evaluation of the arterial lumen and characterization of vessel wall pathologies, and thereby might help in identifying unstable atherosclerotic plaques.

Limitations

The data presented here are exploratory, as the number of animals examined per group was small. Another limitation of our study is the use of semiquantitative scores for histologic evaluation. While quantitative morphometry might yield more accurate results, it crucially relies on consistent staining of all specimens, which was not achieved here due to subsequent processing of the specimens. Another limitation is that the histologic sections are only 5 µm thick while MR slice thickness is 1.5 mm. Therefore, MRI slices represent a projection of 300 possible histological sections, which is why it is never possible to exactly match histology and MRI.

Conclusion

In summary, VSOP iron oxide nanoparticles appear in atherosclerotic plaques within an hour of IV injection of a clinically acceptable dose and are detected by both MRI and histology. VSOP accumulation at 1 hour correlates with the presence of calcifying microvesicles, which are known indicators of inflammatory activity and destabilization of atherosclerotic plaques. We thus experimentally established a new marker–target combination for in vivo characterization of atherosclerotic plaques using electrostatically stabilized VSOP, which thereby is a promising candidate for further clinical development.

Acknowledgments

The authors thank Bettina Herwig for translating the manuscript. This work was funded by the German Research Foundation (DFG), within the Clinical Research Unit KFO 213, BE 1442/8-1, TA 166/3-1, STA 481/1-1.

Disclosure

The authors report no conflicts of interest in this work.

References

1. Schmitz SA, Coupland SE, Gust R, et al. Superparamagnetic iron oxide-enhanced MRI of atherosclerotic plaques in Watanabe hereditable hyperlipidemic rabbits. *Invest Radiol*. 2000;35(8):460–471.
2. Ruehm SG, Corot C, Vogt P, Kolb S, Debatin JF. Magnetic resonance imaging of atherosclerotic plaque with ultrasmall superparamagnetic particles of iron oxide in hyperlipidemic rabbits. *Circulation*. 2001;103(3):415–422.
3. Kooi ME, Cappendijk VC, Cleutjens KB, et al. Accumulation of ultrasmall superparamagnetic particles of iron oxide in human atherosclerotic plaques can be detected by in vivo magnetic resonance imaging. *Circulation*. 2003;107(19):2453–2458.
4. Trivedi RA, U-King-Im JM, Graves MJ, et al. In vivo detection of macrophages in human carotid atheroma: temporal dependence of ultrasmall superparamagnetic particles of iron oxide-enhanced MRI. *Stroke*. 2004;35(7):1631–1635.
5. Sigovan M, Boussel L, Sulaiman A, et al. Rapid-clearance iron nanoparticles for inflammation imaging of atherosclerotic plaque: initial experience in animal model. *Radiology*. 2009;252(2):401–409.
6. Sigovan M, Kaye E, Lancelot E, et al. Anti-inflammatory drug evaluation in ApoE-/- mice by ultrasmall superparamagnetic iron oxide-enhanced magnetic resonance imaging. *Invest Radiol*. 2012;47(9):546–552.
7. Jarrett BR, Correa C, Ma KL, Louie AY. In vivo mapping of vascular inflammation using multimodal imaging. *PLoS One*. 2010;5(10):e13254.
8. Morishige K, Kacher DF, Libby P, et al. High-resolution magnetic resonance imaging enhanced with superparamagnetic nanoparticles measures macrophage burden in atherosclerosis. *Circulation*. 2010;122(17):1707–1715.
9. Woollard KJ, Geissmann F. Monocytes in atherosclerosis: subsets and functions. *Nat Rev Cardiol*. 2010;7(2):77–86.
10. Rogers WJ, Basu P. Factors regulating macrophage endocytosis of nanoparticles: implications for targeted magnetic resonance plaque imaging. *Atherosclerosis*. 2005;178(1):67–73.
11. Tang TY, Patterson AJ, Miller SR, et al. Temporal dependence of in vivo USPIO-enhanced MRI signal changes in human carotid atheromatous plaques. *Neuroradiology*. 2009;51(7):457–465.
12. Makowski MR, Varma G, Wiethoff AJ, et al. Noninvasive assessment of atherosclerotic plaque progression in ApoE-/- mice using susceptibility gradient mapping. *Circ Cardiovasc Imaging*. 2011;4(3):295–303.
13. Morris JB, Olzinski AR, Bernard RE, et al. p38 MAPK inhibition reduces aortic ultrasmall superparamagnetic iron oxide uptake in a mouse model of atherosclerosis: MRI assessment. *Arterioscler Thromb Vasc Biol*. 2008;28(2):265–271.
14. Wilhelm C, Gazeau F. Universal cell labelling with anionic magnetic nanoparticles. *Biomaterials*. 2008;29(22):3161–3174.
15. Fleige G, Seeberger F, Laux D, et al. In vitro characterization of two different ultrasmall iron oxide particles for magnetic resonance cell tracking. *Invest Radiol*. 2002;37(9):482–488.
16. Mallat Z, Hugel B, Ohan J, Lesèche G, Freyssinet JM, Tedgui A. Shed membrane microparticles with procoagulant potential in human atherosclerotic plaques: a role for apoptosis in plaque thrombogenicity. *Circulation*. 1999;99(3):348–353.
17. Li X, Kramer MC, van der Loos CM, et al. A pattern of disperse plaque microcalcifications identifies a subset of plaques with high inflammatory burden in patients with acute myocardial infarction. *Atherosclerosis*. 2011;218(1):83–89.
18. Bobryshev YV, Killingsworth MC, Lord RS, Grabs AJ. Matrix vesicles in the fibrous cap of atherosclerotic plaque: possible contribution to plaque rupture. *J Cell Mol Med*. 2008;12(5B):2073–2082.
19. Hsu HH, Camacho NC, Tawfik O, Sun F. Induction of calcification in rabbit aortas by high cholesterol diets: roles of calcifiable vesicles in dystrophic calcification. *Atherosclerosis*. 2002;161(1):85–94.
20. Taupitz M, Wagner S, Schnorr J, et al. Phase I clinical evaluation of citrate-coated monocrystalline very small superparamagnetic iron oxide particles as a new contrast medium for magnetic resonance imaging. *Invest Radiol*. 2004;39(7):394–405.
21. Wagner M, Wagner S, Schnorr J, et al. Coronary MR angiography using citrate-coated very small superparamagnetic iron oxide particles as blood-pool contrast agent: Initial experience in humans. *J Magn Reson Imaging*. 2011;34(4):816–823.

22. Wagner S, Schnorr J, Pilgrimm H, Hamm B, Taupitz M. Monomer-coated very small superparamagnetic iron oxide particles as contrast medium for magnetic resonance imaging: preclinical in vivo characterization. *Invest Radiol*. 2002;37(4):167–177.
23. Scott JE, Dorling J. Differential staining of acid glycosaminoglycans (mucopolysaccharides) by alcian blue in salt solutions. *Histochemie*. 1965;5(3):221–233.
24. López D, Durán AC, Fernández MC, Guerrero A, Arqué JM, Sans-Coma V. Formation of cartilage in aortic valves of Syrian hamsters. *Ann Anat*. 2004;186(1):75–82.
25. Stary HC, Chandler AB, Dinsmore RE, et al. A definition of advanced types of atherosclerotic lesions and a histological classification of atherosclerosis. A report from the Committee on Vascular Lesions of the Council on Arteriosclerosis, American Heart Association. *Circulation*. 1995;92(5):1355–1374.
26. Virmani R, Kolodgie FD, Burke AP, Farb A, Schwartz SM. Lessons from sudden coronary death: a comprehensive morphological classification scheme for atherosclerotic lesions. *Arterioscler Thromb Vasc Biol*. 2000;20(5):1262–1275.
27. Puchtler H, Meloan SN, Terry MS. On the history and mechanism of alizarin and alizarin red S stains for calcium. *J Histochem Cytochem*. 1969;17(2):110–124.
28. McLachlan SJ, Morris MR, Lucas MA, et al. Phase I clinical evaluation of a new iron oxide MR contrast agent. *J Magn Reson Imaging*. 1994; 4(3):301–307.
29. Li W, Ostblom M, Xu LH, et al. Cytocidal effects of atheromatous plaque components: the death zone revisited. *FASEB J*. 2006;20(13): 2281–2290.
30. Kockx MM, De Meyer GR, Muhring J, Jacob W, Bult H, Herman AG. Apoptosis and related proteins in different stages of human atherosclerotic plaques. *Circulation*. 1998;97(23):2307–2315.
31. Duer MJ, Friscić T, Proudfoot D, et al. Mineral surface in calcified plaque is like that of bone: further evidence for regulated mineralization. *Arterioscler Thromb Vasc Biol*. 2008;28(11):2030–2034.
32. Wexler BC, Judd JT, Kittinger GW. Changes in calcium, hydroxyproline and mucopolysaccharides in various aortic segments of arteriosclerotic breeder rats. *J Atheroscler Res*. 1963;4:397–415.
33. Schnorr J, Wagner S, Abramjuk C, et al. Comparison of the iron oxide-based blood-pool contrast medium VSOP-C184 with gadopentetate dimeglumine for first-pass magnetic resonance angiography of the aorta and renal arteries in pigs. *Invest Radiol*. 2004;39(9):546–553.
34. Taupitz M, Schnorr J, Wagner S, et al. Coronary MR angiography: experimental results with a monomer-stabilized blood pool contrast medium. *Radiology*. 2002;222(1):120–126.
35. Warmuth C, Schnorr J, Kaufels N, et al. Whole-heart coronary magnetic resonance angiography: contrast-enhanced high-resolution, time-resolved 3D imaging. *Invest Radiol*. 2007;42(8):550–557.

Supplementary materials

Animals and tissue processing

Animals were killed in deep anesthesia induced by ketamine hydrochloride and xylazine by a final IV injection of 2 mL T61 (Intervet, Unterschleißheim, Germany). The chest was opened and the aorta flushed via the left ventricle with 200 mL electrolyte solution (Sterofundin®; B. Braun, Melsungen, Germany) with release of blood and fluid via the femoral arteries. Subsequently, the aorta was flushed with 100 mL formaldehyde solution. The complete ascending and descending thoracic aorta was removed, stripped of adjacent connective tissue, and fixed in 5% formaldehyde solution for 48 hours. After fixation, the aortas were cut into 3 mm rings. These rings were embedded in 2% agarose at 40°C doped with 0.1 mL Magnevist (Bayer Healthcare Pharmacueticals, Berlin, Germany) per 100 mL agarose to enhance background signal. Histological processing of the first aortic specimens indicated a link between calcifying vesicles and VSOP, therefore the aortic rings were additionally treated after removal from the agar phantoms using an ethanol formalin fixative for 24 hours (10 mL 40% formaldehyde, 70 mL ethanol absolute, 2 mL glacial acid, 18 mL demineralized water), which is known to improve preservation of calcium deposits in tissues.

Table S1 Definition of AHA lesion types according to Stary et al[1]

AHA lesion type	Definition
I	Initial lesion, single subendothelial foam cells, focal subendothelial GAG accumulation
2	Fatty streak, foci of subendothelial foamy macrophages, beginning confluent GAG accumulation
3	Preatheroma, diffuse intimal thickening consisting of smooth muscle cells in GAG-rich matrix without necrosis or confluent extrcellular lipid
4	Monolayered intimal atheroma, confluent GAG and lipid core, calcium score 0–2, thin cap, low collagen content
5A	Multilayered intimal atheroma, multiple layers of confluent GAG and lipid core, calcium score 0–2, thin cap, low collagen content
5B	Multilayered intimal atheroma, multiple layers of confluent GAG and lipid core, calcium score 3, thin cap, low collagen content
5C	Multilayered fibrotic lesion, collagen-rich lesion with minor lipid or GAG pools, calcium score 0–3
6	Erosion, hemorrhage, endothelial surface thrombosis

Abbreviations: AHA, American Heart Association; GAG, glycosaminoglycan.
Note: Copyright © 2000, Walter Kluwer Health. Adapted with permission from Virmani R, Kolodgie FD, Burke AP, Farb A, Schwartz SM. Lessons from sudden coronary death: a comprehensive morphological classification scheme for atherosclerotic lesions. *Arterioscler Thromb Vasc Biol*. 2000;20(5):1262–1275.[2]

Staining procedures

The histological specimens were stained using the following procedures:

1. Overall morphology: Movat pentachrome stain (stains file and proprietary stains kit from Morphisto [Frankfurt, Germany]).
2. Calcium deposits: von Kossa stain and, in selected specimens, Alizarin S at pH 4.2 and pH 6.4 and Alizarin at pH 11.
3. Iron deposits: Prussian blue, 2% potassium ferrocyanide solution in 1% hydrochloric acid with a counterstain of acid fast red (preparation by cooking with aluminum sulfate and filtration) and, in selected specimens, 1% potassium ferrocyanide solution in 0.5% hydrochloric acid.

Table S2 Scoring system for morphologic and histopathologic analysis of vessel segments by microscopic field of view using ×200 magnification

Criterion	Stain	Measurements/scores
Integrity of media	Anti-SMA	0: no loss of SMC layers 1: <50% loss of media 2: >50% loss of media 3: <5 layers of media remaining
Intimal smooth muscle cell proliferation	Anti-SMA	0: no SMC in intima 1: up to 5 SMC layers in intima 2: 5–10 SMC layers in intima 3: >10 SMC layers in intima
Microvesicles	Movat pentachrome	0: no blue bodies 1: up to 10 blue bodies 2: up to 20 blue bodies 3: >20 blue bodies
Calcification	von Kossa (Alizarin)	0: no black–brown (purple) structures 1: up to 100 black–brown (purple) spots 2: >100 black–brown (purple) spots 3: confluent black–brown (purple) areas
Ferric iron	Prussian blue	0: no blue spots 1: up to 20 blue spots 2: up to 50 blue spots 3: >50 blue spots
Macrophages	Anti-RAM-11	0: no red-stained structures 1: up to 10 red foci 2: up to 20 red foci 3: >20 red foci
Angiogenesis	Anti-VEGF	0: no red-stained structures 1: up to 10 red foci 2: up to 20 red foci 3: >20 red foci

Abbreviations: RAM-11, rabbit macrophage clone RAM-11; SMA, smooth muscle cell actin; SMC, smooth muscle cell; VEGF, vascular endothelial growth factor.

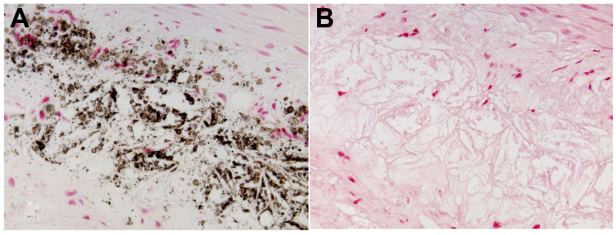

Figure S1 Intimomedial area of an atherosclerotic lesion of a WHHL rabbit without VSOP injection. Despite the presence of numerous calcifying microvesicles in the von Kossa stain (**A**), the microvesicles appear pink in the Prussian blue stain (**B**), indicating absence of stainable amounts of iron.
Abbreviations: VSOP, very small superparamagnetic iron oxide particles; WHHL, Watanabe heritable hyperlipidemic.

4. Macrophages: rabbit anti-macrophage antibody (anti-RAM, mouse anti-rabbit, anti-RAM-11Ab-5; dianova, Hamburg Germany) at a dilution of 1:100.
5. Smooth muscle cell actin: anti-actin antibody (anti-SMC, mouse anti-human clone 1A4; Dako, Hamburg, Germany), dilution of 1:200.
6. Vascular endothelial growth factor (VEGF): anti-VEGF antibody (anti-vascular endothelial growth factor, mouse anti-human, rabbit VEGF Ab-3 [JH121]; dianova).
7. Glycosaminoglycans: selected specimens with high number of microvesicles in Movat stain were stained using the critical electrolyte concentration method with 0.05% Alcian 8GX in a 0.05 M acetate buffer at pH 5.8 and a 0.44 M magnesium chloride concentration and counterstaining with neutral red (0.5%).

All antibodies were diluted in da Vinci green (Biocare Medical, Concord, CA, USA). Goat anti-mouse IgG (Nobel Biocare) was used as secondary antibody; after coupling with streptavidin horseradish peroxidase (Nobel Biocare), red color was developed using an aminoethyl carbazole substrate kit (Zymed Labs, San Fransisco, CA, USA) with blue counterstain using hematoxylin. Immunohistochemistry was performed by Labor Habedank (Großziethen, Germany).

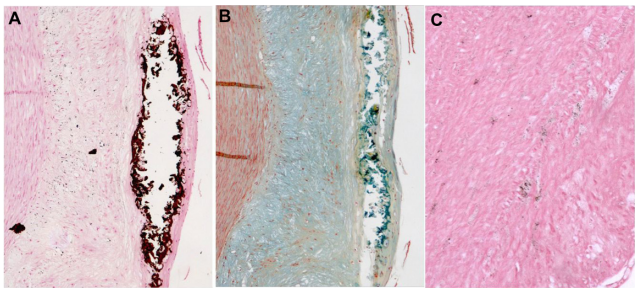

Figure S2 Colocalization of confluent calcification in the von Kossa stain (**A**) with intense blue, alcianophilic deposits in the Movat stain (**B**). Faint calcium deposits in the von Kossa stain in the media (**C**).

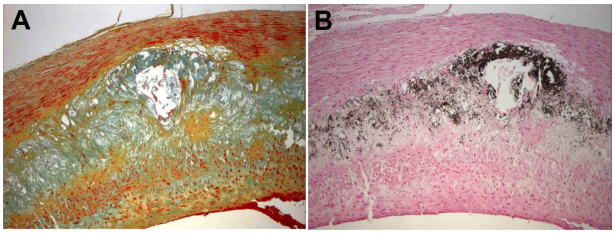

Figure S3 Colocalization of blue-stained alcionophilic material in the Movat pentachrome stain (**A**) and calcification in the von Kossa stain (**B**) indicating a link between GAGs and calcification.
Abbreviation: GAGs, glycosaminoglycans.

References

1. Stary HC, Chandler AB, Dinsmore RE, et al. A definition of advanced types of atherosclerotic lesions and a histological classification of atherosclerosis. A report from the Committee on Vascular Lesions of the Council on Arteriosclerosis, American Heart Association. *Circulation*. 1995;92(5):1355–1374.
2. Virmani R, Kolodgie FD, Burke AP, Farb A, Schwartz SM. Lessons from sudden coronary death: a comprehensive morphological classification scheme for atherosclerotic lesions. *Arterioscler Thromb Vasc Biol*. 2000;20(5):1262–1275.